Structural Relaxation of Langmuir−Blodgett Films of Poly(vinyl octanal acetal) with Various Tacticities

Michiaki Mabuchi, Kenji Kawano, Shinzaburo Ito, and Masahide Yamamoto*

Department of Polymer Chemistry, Graduate School of Engineering, Kyoto University, Yoshida, Sakyo, Kyoto 606-8501, Japan

Received March 3, 1998; Revised Manuscript Received June 7, 1998

ABSTRACT: Poly(vinyl octanal acetal) (PVO) was prepared from poly(vinyl alcohol) (PVA) in which the main chain had three different tacticities and the stereoregularity was characterized by ^{1}H NMR spectroscopy. *a*-PVO prepared from *atactic*-PVA and *s*-PVO from *syndiotactic*-PVA had similar fractions of *cis*- and *trans*-acetals in the main chain, but *i*-PVO from *isotactic*-PVA had different ones. Ultrathin films of these polymers were prepared by the Langmuir−Blodgett (LB) technique, and the thermal relaxation of their multilayer structure was investigated by the energy-transfer method. When the LB films were composed of polymers which had a main chain with a similar stereostructure, the polymers were intermingled with each other by the thermal treatment and the onset of the diffusion of polymer segments was affected by the glass-transition temperature of the bulk. In contrast, the polymers with different stereostructures in each layer were not mixed with each other, but phase-separated, presumably forming droplets in the ultrathin films. It is concluded that the relaxation behavior of polymer LB films strongly reflects the stereoregularity of the sample polymers.

Introduction

Ultrathin films have been studied extensively in the field of applications such as electronics and optics during the past decade.[1] Many kinds of polymers are known to provide a thermally and mechanically stable ultrathin LB film compared with the low-molecular-weight amphiphilic compounds.[2−7] The characteristics of polymer LB films are, for example, thinness of each layer (1−2 nm/layer), fewer defects such as pinhole, and durability of the films, all of which are desirable properties for the application. Another advantage of polymer LB films is the possibility of a greater variety of structure. Various physical properties can be given to the obtained film by changing the chemical structure of the monomer unit, molecular weight of the polymer, and stereostructure of the main chain. For example, Schouten et al. reported a series of studies on the monolayer behavior for poly(methyl methacrylate) and the structure of its LB film.[8] The orientational characteristics of the crystalline structure in the film strongly depend on the tacticity, molecular weight, and also history of the monolayer before the deposition.

From the view of application of LB films, durability of the deposited structure is one of the most important properties. Thus, it is necessary to know the mechanism of the structural relaxation of the LB films. We have studied the layered structure of poly(vinyl octanal acetal) (PVO) LB films and its thermal relaxation behavior through the interlayer energy transfer.[9−15] The energy-transfer method is a powerful one to observe the structures in a molecular dimension. Previously, the effect of side chain length[13] and that of molecular weight[14] on the structural relaxation have been reported. This paper focuses on the effect of the main chain structure on the relaxation behavior in PVO as a sample polymer. PVO is an excellent LB material because of its good transferability in a wide range of conditions.[8] Besides, it is also useful as a base polymer to which various kinds of fluorescent moieties can be introduced as a side chain.[9] PVOs with various tacticities were prepared and the thermal stability of the LB films was investigated by the energy-transfer method.

Chart 1. Chemical Structure of Poly(vinyl octanal acetal) PVO

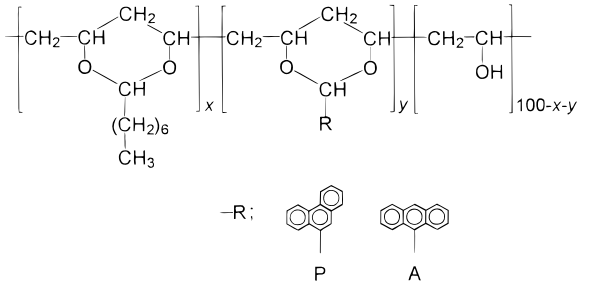

Experimental Section

Materials and Characterization. PVOs (Chart 1) were synthesized by acetalization of poly(vinyl alcohol) (PVA) s with three different tacticities of the main chain, isotactic (*i*-PVA), atactic (*a*-PVA), and syndiotactic (*s*-PVA). These are named as *i*-PVO, *a*-PVO, and *s*-PVO, respectively. The detailed procedure for the synthesis was described previouly.[10] *i*-PVA and *s*-PVA were kindly gifted by Kuraray Co. Ltd. *a*-PVA was purchased from Wako Pure Chemical Industries. Each sample has the same degree of polymerization: 2000. The polymer was labeled with phenanthrene (P) or anthracene (A) chromophores by the acetalization of diols with the corresponding chromophoric aldehyde (Aldrich). Compositions of the prepared polymers were determined from the carbon fraction by the elemental analysis, and from UV absorption of the chromophoric moiety in dichloromethane.

PVAs for the ^{1}H NMR measurement were purified by reprecipitation from benzene into methanol three times. ^{1}H NMR spectra of PVAs in dimethyl sulfoxide-d_6 (DMSO) were measured by a FT-NMR spectrometer (JEOL; 90 MHz). ^{1}H NMR measurement of PVOs in chloroform-d_1 was carried out using a 400-MHz NMR spectrometer (JEOL).

Preparation of LB Films. A nonfluorescent quartz plate for the substrate was cleaned with oxidative sulfuric acid, rinsed with pure water, and then made hydrophobic by dipping into a 10% toluene solution of trimethylchlorosilane for 30 min.

S0024-9297(98)00336-2 CCC: $15.00
Published on Web 08/21/1998

Table 1. Compositions, Glass-Transition Temperatures, and Surface Pressures for the LB Deposition of PVOs

sample	x (%)	y (%)	$100 - x - y$ (%)	T_g (°C)	surface pressure (mN m^{-1})
i-PVO	68		32	12	18.0
i-PVO−P	63	9.0	28	33	14.0
i-PVO−A	74	4.0	22	18	17.0
a-PVO	67		33	23	23.0
a-PVO−P	57	12	31	50	17.5
a-PVO−A	55	7.0	38	48	20.0
s-PVO	61		39	19	23.5
s-PVO−P	57	9.0	34	47	17.5
s-PVO−A	59	4.0	37	40	20.0

Water for the subphase was purified by deionization, distillation, and filtration through a water purification column (Barnstead Nanopure II). A benzene (Dojin, spectrograde) solution of the sample polymer (0.1 wt %) was spread on pure water in a Teflon-coated trough (Kenkosha Model SI-1) and the solvent was allowed to evaporate. The temperature of the subphase was maintained at 19 °C. The monolayer had been compressed at a rate of 10 mm min^{-1} to an appropriate surface pressure (see Table 1). The vertical transfer onto a substrate was performed at the deposition velocity of 15 mm min^{-1}. All the monolayers were transferable as Y-type films with good transfer ratios around unity. The surface pressure−area isotherms were measured under the same conditions.

Figure 1a shows the structure of the LB films for the energy-transfer measurements. The energy-donating layers of P-labeled PVO and the energy-accepting layers of A-labeled PVO were sandwiched by the matrix layers of nonchromophoric PVO. The distance between the energy-donating layers and the -accepting layers was controlled by altering the number of spacing layers n (n = 0, 4). To compare the relaxation process under the same conditions, the total number of layers was kept at 18 by adjusting the number of protection layers. Figure 1b depicts the tacticities of each layers. The sample films in which all layers consist of the same tactic polymers are abbreviated as *aa-n*, *ii-n*, and *ss-n* for atactic, isotactic, and syndiotactic ones, respectively, where *n* is the number of spacing layers mentioned above. Samples with different tacticities were also prepared; *a*-PVOs labeled with P or A chromophores were used as the probing layers, and *s*-PVO, or *i*-PVO, was used as the matrix layers. They are abbreviated as *as-n* and *ai-n*, respectively. After the deposition, the LB film was allowed to dry in a desiccator overnight and stored in a refrigerator until the measurements.

Energy-Transfer Measurements. Fluorescence spectra of LB films were recorded by a Hitachi 850 fluorescence spectrophotometer equipped with a thermoregulated sample chamber. Phenanthrene chromophores in the film were excited selectively by 298-nm light, at which the excitation probability of A was less than 5% of P. The spectral change under the thermal treatment was measured, with a constant heating or cooling rate of 0.5 °C min^{-1} in the range of 30−100 °C.

Results and Discussion

Tacticity of Polymers. ^{1}H NMR spectroscopy was used to determine the tacticity of PVA.[16−21] Although the diad and triad tacticities of PVA have been studied by the methylene and methine protons on NMR spectra, respectively,[16−19] these peaks have poor resolution for a quantitative analysis. Then the hydroxyl proton signals were employed for the determination of tacticity.[20,21] The NMR spectrum of PVA dissolved in DMSO shows three well-resolved triad peaks at 4.10, 4.33, and 4.52 ppm of chemical shift, being assigned to a syndiotactic, heterotactic, and isotactic triad, respectively. The tacticities of PVA samples were obtained from the areas of these peaks as shown in Table 2.

In the acetalization reaction, an aldehyde molecule (1-octanal) reacts with two adjacent hydroxyl groups on a PVA chain to form two types of acetal rings, depending on the diad of the hydroxyl units. These are *cis*-4,6-substituted 1,3-dioxane ring (called *cis*-acetal) formed from an isotactic part of a PVA chain and *trans*-4,6-substituted 1,3-dioxane ring (*trans*-acetal) from a syndiotactic part. Figure 2 shows their stereostructures.

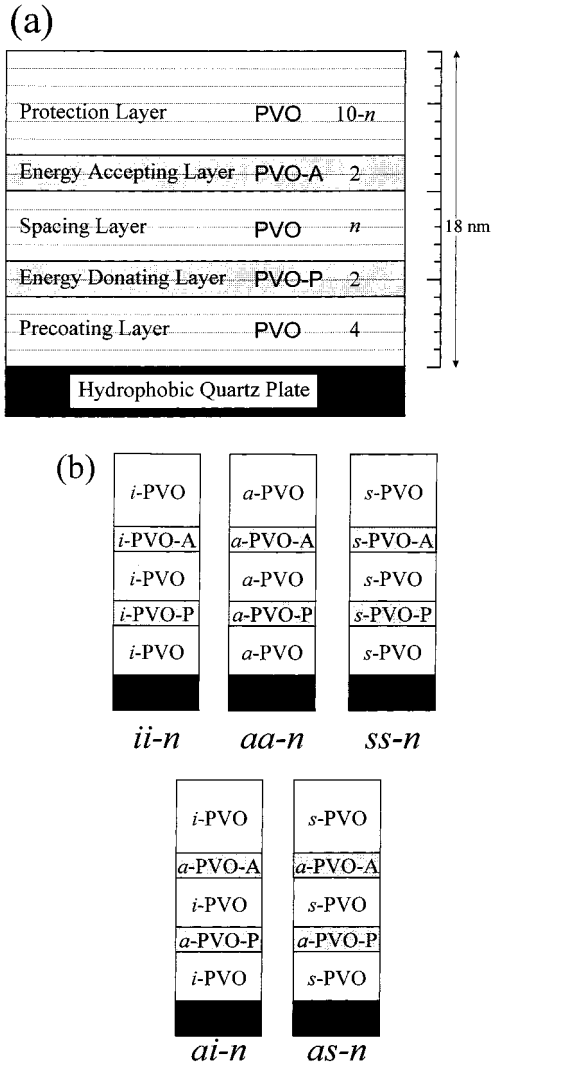

Figure 1. (a) Schematic illustration of layer structure of LB films for the energy transfer measurement. The letter *n* means the number of the spacing layers, 0 or 4. (b) The tacticities of each layers.

Table 2. Tacticities of PVAs Used as Source Polymers for PVO Synthesis

	triad (%)			diad (%)	
sample	isotactic	heterotactic	syndiotactic	isotactic	syndiotactic
i-PVA	76.7	19.6	3.70	86.5	13.5
a-PVA	21.6	46.4	32.0	44.8	55.2
s-PVA	10.8	52.3	36.9	36.9	63.1

Fractions of *cis*-acetal and *trans*-acetal in a synthesized PVO chain were also determined by ^{1}H NMR spectroscopy as shown in Figure 3.[7a,22−26] By a comparison of the spectra with those of poly(vinyl formal)s, the peaks in the range of 4.8−3.7 ppm were assigned as follows:[25] (1) 4.75 ppm, methine proton of H_b' in the *trans*-acetal ring; (2) 4.5 ppm, methine proton of H_b in *cis*-acetal; (3) 4.4−3.7 ppm, methine protons of H_a and H_a' in both acetals and hydroxyl protons of the unacetalized PVA part. Therefore, the methine protons H_b

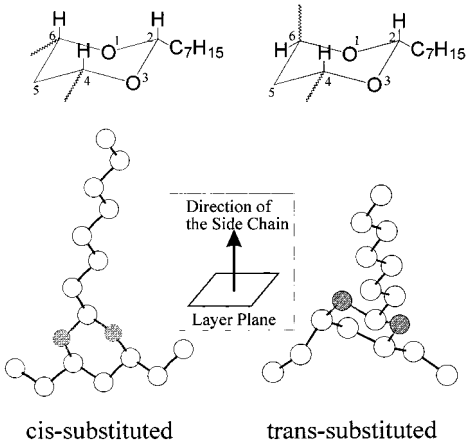

Figure 2. Stereostructure of *cis* and *trans*-4,6-substituted 1,3-dioxane ring in the PVO main chain: (left) *cis*-substituted; (right) *trans*-substituted. In the molecular model shown in the bottom, the molecules are placed assuming that the main chain lies on the layer plane and the side chain, octyl group orients in the direction normal to the plane.

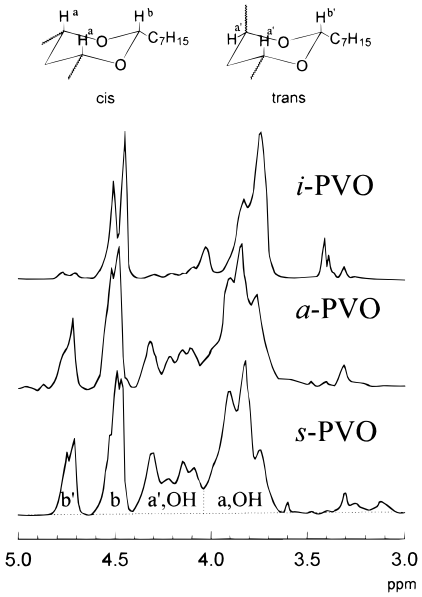

Figure 3. 400 MHz ^{1}H NMR spectra of PVOs chloroform-d_1 solutions, which are measured at 55 °C.

Table 3. Tacticities of PVOs Evaluated from ^{1}H NMR

sample	*cis*-acetal	*trans*-acetal
i-PVO	95.0	5.00
a-PVO	70.7	29.3
s-PVO	67.7	32.3

and H_b' could be utilized to determine the fraction of the stereostructure of acetal rings. Obtained values are listed in Table 3. *i*-PVO bears mostly *cis*-acetal, but *a*-PVO and *s*-PVO have similar compositions of *cis*- and *trans*-acetal despite the different tacticities in the original PVA. From the comparison of Tables 2 and 3, the fraction of *cis*-acetal is much greater than that of the isotactic diad in the starting PVA. This indicates that acetalization proceeds more preferentially at the isotactic diad than at the syndiotactic diad. Shibatani et al. demonstrated that the migration of the acetal ring from syndiotactic to isotactic hydroxyl groups occurs in the long time reaction. This means that *cis*-acetal is more stable kinetically and also thermodynamically than *trans*-acetal.[22]

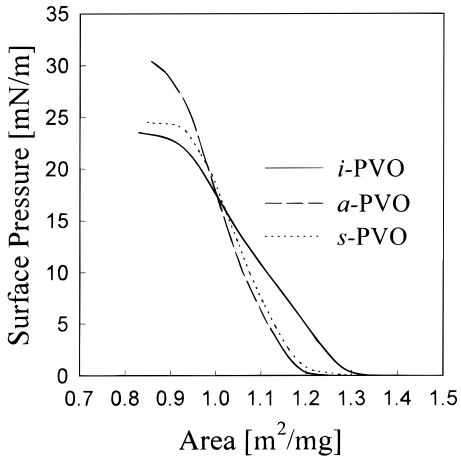

Figure 4. Surface pressure−area isotherms of PVOs measured at 19 °C.

Monolayer Properties. Figure 4 depicts the surface pressure−area isotherms of *i*-PVO, *a*-PVO, and *s*-PVO. The monolayer of *i*-PVO gave a larger limiting area than that of the other PVOs. This result is attributed to the rigid structure of the *i*-PVO main chain. As shown in Figure 2, the main chain, which is a part of the 1,3-dioxane ring, is likely to bend at the *trans*-acetal. In contrast, the main chain at the *cis*-acetal part must be linear, consequently, relatively rodlike for a *cis*-rich configuration. Therefore, the *i*-PVO chain, having a high content of the *cis*-acetal ring, is more difficult to be packed with neighboring chains on the two-dimensional plane of the water surface, giving rise to an appreciable surface pressure even in the lower extent of packing compared with the *s*- or *a*-PVO chains. Similar phenomena have been reported in the monolayer of *isotactic* poly(methyl methacrylate).[8,27]

Thermal Stability of Multilayer Structure Measured by the Energy-Transfer Method. The structural change in ultrathin films could be well-detected by the energy-transfer technique. Labeling with a small amount of chromophores (a few mol %) is enough to give a sufficient intensity of fluorescence from the ultrathin films. In addition, because the energy transfer rate is determined by the inverse sixth power of the distance between donor and acceptor molecules,[28] the transfer efficiency reflects a small alteration of distances in the scale of a few nanometers.

Figure 5 shows the fluorescence spectra of the *aa*-4 LB film before and after the thermal treatment. At the beginning, the energy-donating layers and the energy-accepting layers were separated approximately 4 nm apart since the thickness per layer is 1.02 nm by ellipsometry.[7a] The Förster radius for the P−A pair is 2.12 nm;[29] thus, the interlayer energy transfer from P to A does not occur sufficiently, yielding P-dominant emission on the spectrum. However, after the thermal treatment, the spectra were markedly changed; the intensity of A emission at 438 nm (I_A) became higher and that of P emission at 350 nm (I_P) became lower. The thermal treatment gave rise to considerable change of I_A/I_P but no appreciable wavelength shift on both absorption and fluorescence spectra. This indicates that the P-labeled layers became closer to the A-labeled layers than those in the initial state by the disordering of the layered structure. Therefore, by monitoring the energy-transfer efficiency, one can probe the structural relaxation of the LB films. Here, the ratio I_A/I_P was

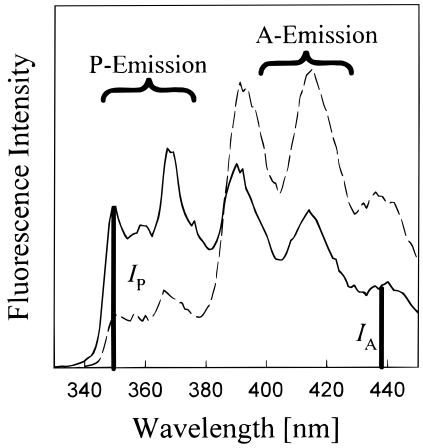

Figure 5. Spectral change of *aa*-4 films with a constant temperature, 60 °C for 7 h: (solid line) before heating; (dashed line) after heating. The excitation wavelength is 298 nm.

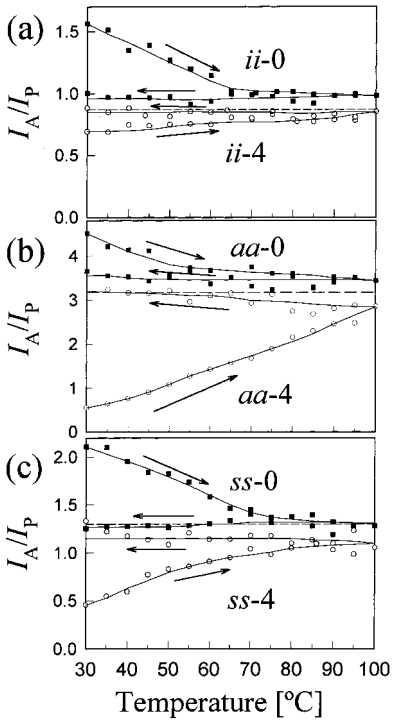

Figure 6. The change of the energy-transfer efficiency of PVO LB films with homogeneous tacticity under the heating/cooling: (a) *ii*-*n*, (b) *aa*-*n*, and (c) *ss*-*n*. The calculated value of I_A/I_P under the uniform distribution of the chromophores is shown by a dashed line.

used as an appropriate measure of the energy-transfer efficiency. A trace amount of P emission at 438 nm was subtracted from the I_A actually observed.

Structural Relaxation of LB Films Prepared from PVOs with Similar Tacticity. Figure 6 shows the change of I_A/I_P on the first run of heating and cooling. The values of I_A/I_P are plotted against temperature; thus, the alteration shows a structural relaxation of the LB multilayer. Since the observed temperatures are already higher than T_g of the matrix PVO, the segmental motion of the polymer main chain is active, giving rise to disordering of the layer. The I_A/I_P increased for $n = 4$ and decreased for $n = 0$. The final values of I_A/I_P (i.e., in equilibrium) were almost the same regardless of n. Once reaching this value, the I_A/I_P did not change any further during the successive cooling or heating process. Differences in the saturated values among the samples are attributed to the different contents of P and A chromophores in the probing layers. The value of I_A/I_P after the sufficient thermal treatment indicates that the layered structure of the LB films was disordered irreversibly to a stable state in which all components were completely mixed.

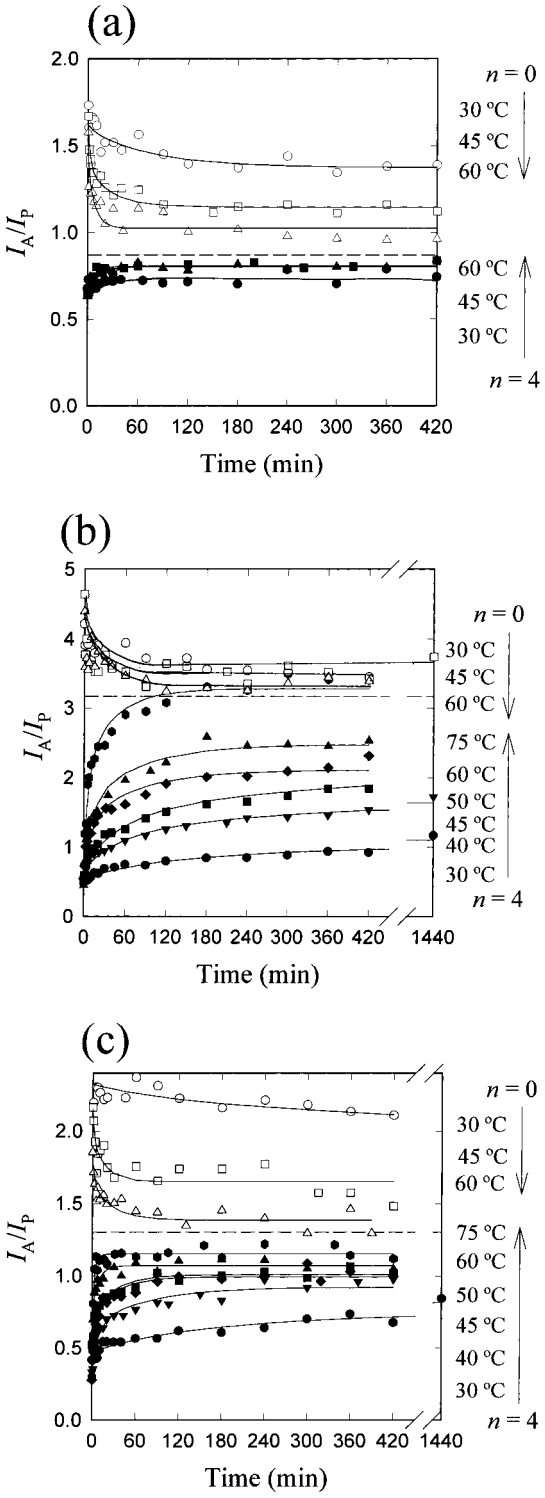

Figure 7. The energy-transfer efficiency as a function of time at various temperatures: (a) *ii*-*n*, (b) *aa*-*n*, and (c) *ss*-*n*.

Figure 7 shows the time dependence of I_A/I_P under constant temperatures. Theoretical calculations based on Förster kinetics were applied to analyze the diffusion of polymer segments, assuming time-dependent Gaussian distributions of chromophores in the direction

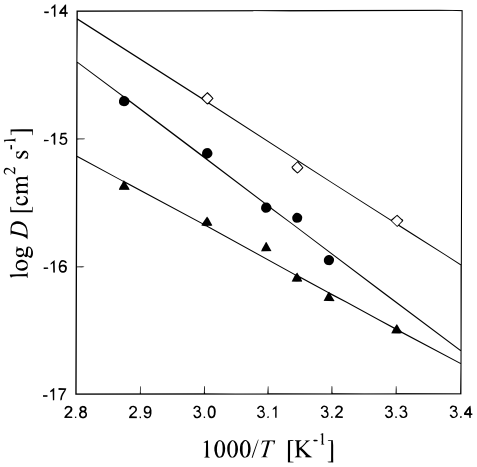

Figure 8. Arrhenius plot of diffusion constant D: (◇) *i*-PVO, (▲) *a*-PVO, and (●) *s*-PVO.

normal to the layer plane. The details of the computer simulation have been described previously.[12,13] Fitting of the theoretical curve to the time-dependent energy-transfer efficiency allowed us to evaluate the diffusion constant D for the LB films. Obtained values of D were plotted in Figure 8.

The D values for the three PVOs are in the increasing order of *a*-PVO, *s*-PVO, and *i*-PVO, which is the same order as the T_g values in the bulk. The lower T_g leads to the larger diffusivity of the polymer segments in the film when compared at a fixed temperature. It is reasonable that the polymer chain has similar mobility or flexibility both in a polymer bulk and in an LB film. The result shows that the relaxation properties of polymer ultrathin films are closely related to those of the bulk polymers. In addition, if each layer on a water surface is transferred onto the substrate, keeping its monolayer structure, a larger diffusivity of *i*-PVO than those of other PVOs is expected from the surface pressure−area isotherm. The *i*-PVO film is sparsely packed so that it is easy to diffuse into free space when the segmental motion is allowed by the thermal effect.

As shown in Figure 8, the Arrhenius plot of D gave a straight line in the range of observed temperatures. From the slope of the plot, the apparent activation energy for the relaxation of the ultrathin LB films, ΔE_a, was calculated by eq 1:

$$D = D_0 \exp\left(-\frac{\Delta E_a}{RT}\right) \quad (1)$$

The values of ΔE_a for *ii*-4, *aa*-4, and *ss*-4 were 61, 52, and 72 kJ mol^{-1}, respectively. Considering the experimental error and temperature dependence of ΔE_a, these values are roughly in the same range. The ΔE_a values for poly(vinyl pentanal acetal) and poly(vinyl butanal acetal) in the same temperature range are 120 and 110 kJ mol^{-1},[13b] respectively. Both polymers, having shorter alkyl side chains, showed a much larger ΔE_a. This suggests that the effect of the side chain length on ΔE_a is larger than the effect of tacticity.

Structural Relaxation of the Films with Different Tacticities. Figure 9 shows the change of I_A/I_P for *as-n* and *ai-n* samples. In *as-n* samples, as in *aa-n*, mixing of each layer was observed after heating. On the other hand, *ai-n* samples exhibited a strange behavior; a slight increase of I_A/I_P was observed even in the case of $n = 0$. After the samples were heated

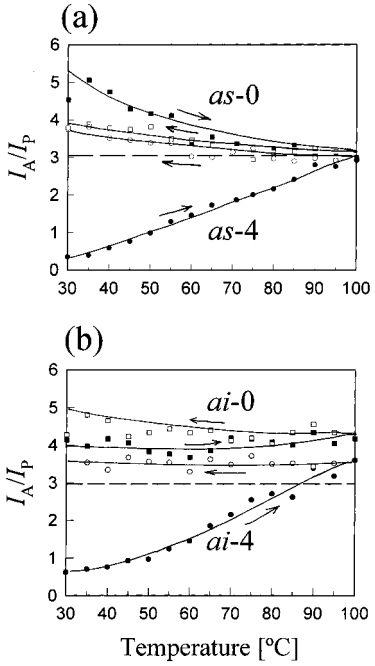

Figure 9. The change of the energy-transfer efficiency of PVO LB films with heterogeneous tacticities under the heating/cooling: (a) *as-n*; (b) *ai-n*. The calculated value of I_A/I_P under the uniform distribution of the chromophores is shown by a dashed line.

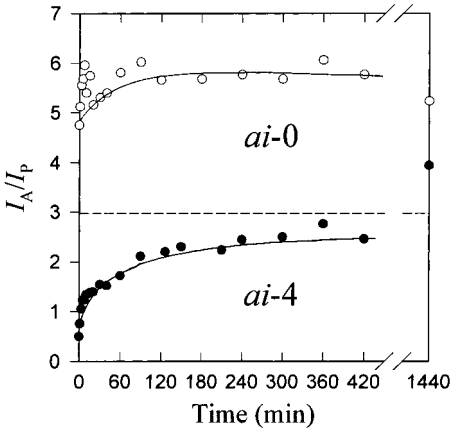

Figure 10. The energy-transfer efficiency of *ai-n* LB film as a function of time at 60 °C.

around 100 °C, the I_A/I_P values in $n = 0$ and 4 became constant, but they were different. Both of them were larger than the calculated value for the model that all the layers were intermingled. Figure 10 shows the change of I_A/I_P for *ai-n*, plotted against the time when the sample was kept at a constant temperature, 60 °C. The increase of I_A/I_P was also observed for both samples of *ai*-0 and *ai*-4. Apparently, the final state in *ai-n* is not the same as that in the previous systems.

This behavior can be explained by the phase separation of probing PVO from the matrix PVO.[15] A mixture of immiscible polymers is known to be phase-separated in equilibrium. The phase separation arises from the structural difference between them. Chromophoric PVO (atactic) and matrix PVO (isotactic) have different stereostructures in the main chain, as described in the previous section. When the probe polymer is incompatible with the matrix polymer, the polymer is likely to form a droplet to minimize the surface energy. Continuous heat treatment will accelerate the growth of

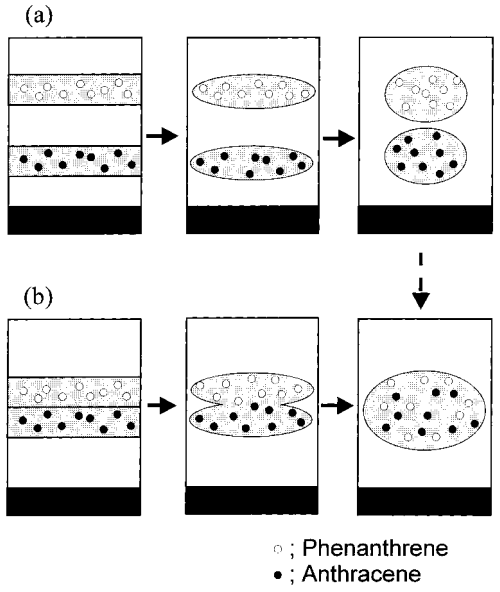

Figure 11. Schematic presentation of the structural relaxation of *ai*-*n* LB films: (a) *ai*-4; (b) *ai*-0. To clarify the concept, only P and A chromophores are drawn and the polymer chains were omitted.

droplets involving the aggregation of both *a*-PVO−P and *a*-PVO−A. Consequently, P and A chromophores are concentrated in the domain of *a*-PVO, yielding a high transfer efficiency compared with the homogeneous distribution of chromophores over the whole matrix film. The different states of *ai*-0 and *ai*-4 after the relaxation can be derived from the miscibility of layers and from the different initial layer structures. As for *ai*-0, the probing polymers *a*-PVO−P and *a*-PVO−A are in contact with each other, and these polymers easily aggregate when mutual diffusion is allowed in the film. On the contrary, the probing polymers are separated for *ai*-4 film before relaxation. Therefore, the thermal relaxation of layers yields P- and A-labeled polymer droplets separately as schematically shown in Figure 11. The very slow relaxation process (denoted by the dashed arrow in Figure 10) may proceed to provide the same state as the terminal state of *ai*-0 after a sufficiently long time. These findings indicate that the relaxation behavior through the miscibility of polymers strongly depends on the stereostructure of the main chain.

Conclusion

Thermal relaxation of PVO LB films with various tacticities was measured by using the energy-transfer phenomenon from a P-labeled polymer to an A-labeled polymer. The as-deposited structure in which a polymer chain was confined in a quasi two-dimensional array was relaxed by the thermal treatment above T_g of the polymer bulk. After the thermal treatment, the miscible LB films exhibited a random distribution of polymer chains, whereas immiscible LB films induced a phase separation of the probing polymers from the matrix polymer. The miscibility of the layers depended on the stereostructure of the polymer; when the probing layers and the matrix layers were composed of polymers with the same or similar stereoregularity, the layers were easily intermingled in the film. The thermal hysteresis of the energy-transfer efficiency was well-characterized by the miscibility of the LB films and also the diffusion rate of each polymer. Thus, the relaxation behavior of the ultrathin films is strongly governed by the stereostructure of the polymer main chain.

Acknowledgment. The present study was supported by a Grant-in-Aid for Science Research (No. 09450360) from the Ministry of Education, Science, Sports, and Culture of Japan.

References and Notes

(1) Ulman, A. *An Introduction of Ultrathin Organic Films from Langmuir−Blodgett to Self-Assembly*; Academic Press: San Diego, CA, 1991; Part 2.
(2) Tredgold, R. H.; Winter, C. S. *J. Phys. D.; Appl. Phys.* **1982**, *15*, L55. (b) Tredgold, R. H.; Winter, C. S. *Thin Solid Films* **1983**, *99*, 81. (c) Tredgold, R. H. *Thin Solid Films* **1987**, *152*, 223.
(3) Breton, T. *J. Macromol. Sci., Rev. Macromol. Chem.* **1981**, *C21*, 1326.
(4) Miyashita, M. *Prog. Polym. Sci.* **1993**, *18*, 263.
(5) Duda, G.; Schouten, A. J.; Arndt, T.; Lieser, G.; Schmidt, G. F.; Bubeck, C.; Wegner, G. *Thin Solid Films* **1988**, *159*, 221. (b) Orthmann, E.; Wegner, G. *Makromol. Chem., Rapid Commun.* **1986**, *7*, 243. (c) Wegner, G. *Thin Solid Films* **1992**, *216*, 105.
(6) Embs, F.; Funhoff, D.; Laschewski, A.; Licht, U.; Ohst, H.; Prass, W.; Ringsdorf, H.; Wegner, G.; Wehrmann, R. *Adv. Mater.* **1991**, *3*, 25.
(7) Watanabe, M.; Kosaka, Y.; Oguchi, K.; Sanui, K.; Ogata, N. *Macromolecules* **1988**, *21*, 2997. (b) Oguchi, K.; Yoden, T.; Kosaka, Y.; Watanabe, M.; Sanui, K.; Ogata, N. *Thin Solid Films* **1988**, *161*, 305.
(8) Schouten, A. J.; Brinkhuis, R. H. G. *Macromolecules* **1991**, *24*, 1487. (b) Schouten, A. J.; Brinkhuis, R. H. G. *Macromolecules* **1991**, *24*, 1496.
(9) Ito, S.; Okubo, H.; Ohmori, S.; Yamamoto, M. *Thin Solid Films* **1989**, *179*, 445. (b) Ohmori, S.; Ito, S.; Yamamoto, M.; Yonezawa, Y.; Hada, H. *J. Chem. Soc., Chem. Commun.* **1989**, 1293.
(10) Ohmori, S.; Ito, S.; Yamamoto, M. *Macromolecules* **1991**, *24*, 2377.
(11) Ueno, T.; Ito, S.; Ohmori, S.; Onogi, Y.; Yamamoto, M. *Macromolecules* **1992**, *25*, 7150.
(12) Hayashi, T.; Okuyama, T.; Ito, S.; Yamamoto, M. *Macromolecules* **1994**, *27*, 2270.
(13) Yamamoto, M.; Kawano, K.; Okuyama, T.; Hayashi T.; Ito, S. *Proc. Jpn. Acad.* **1994**, *70(B)*, 121. (b) Mabuchi, M.; Kawano, K.; Ito, S.; Yamamoto, M.; Takahashi, M.; Masuda, T. *Macromolecules* **1998**, *31*, 6083.
(14) Ito, S.; Kawano, K.; Hayashi, T.; Yamamoto, M. *Polym. J.* **1996**, *28*, 164.
(15) Hayashi, T.; Ito, S.; Onogi, Y.; Yamamoto, M.; Matsumoto, A. *Eur. Polym. J.* **1994**, *27*, 2270.
(16) Bargon, V. J.; Hellwege, K. H.; Johnsen, U. *Makromol. Chem.* **1965**, *85*, 291.
(17) Ramey, K. C.; Field, N. D. *J. Polym. Sci., Part B* **1965**, *3*, 63. (b) Ramey, K. C.; Field, N. D. *J. Polym. Sci., Part B* **1965**, *3*, 69.
(18) Danno, A.; Hayakawa, N. *Bull. Chem. Soc. Jpn.* **1962**, *35*, 1748.
(19) Tincher, W. C. *Makromol. Chem.* **1965**, *85*, 46.
(20) Moritani, T.; Kuruma, I.; Shibatani, K.; Fujiwara, Y. *Macromolecules* **1972**, *5*, 577.
(21) Hu, S.; Horii, F.; Odani, H. *Bull. Inst. Chem. Res., Kyoto Univ.* **1990**, *67*, 239.
(22) Shibatani, K.; Fujii, K.; Oyanagi, Y.; Ukida, J.; Matsumoto, M. *J. Polym. Sci., Part C* **1968**, *23*, 647.
(23) Pollers, I.; Adriaensens, P.; Carleer, R.; Vanderzande, D.; Gelan, D. *Macromolecules* **1996**, *29*, 5875.
(24) Chanda, M.; Kumar, V. *Angew. Makromol. Chem.* **1977**, *62*, 229.
(25) Shibatani, K.; Fujii, K. *J. Polym. Sci., Part A-1* **1970**, *8*, 1647.
(26) Smets, G.; Petit, B. *Makromol. Chem.* **1959**, *33*, 41.
(27) Kuan, S. W.; Fabian, R.; Pease W.; Frank, C. W. *Polymers for Microelectronics*; Tabata, Y., Mita, I., Nonogaki, S., Eds.; Kodansha: Tokyo, 1990; p 169.
(28) Förster, Th. *Z. Naturforsch., A: Phys. Sci.* **1949**, *4*, 321.
(29) Berlman, I. B. *Energy Transfer Parameters of Aromatic Compounds*; Academic Press: New York, 1973.

MA980336H